9314 *Macromolecules* **2004,** *37,* 9314−9320

Homogeneous Tandem Catalysis of Bis(2-decylthioethyl)amine−Chromium Trimerization Catalyst in Combination with Metallocene Catalysts

Deon de Wet-Roos* and John Thomas Dixon

Sasol Technology (Pty) Ltd., R&D Division, 1 Klasie Havenga Road, Sasolburg, South Africa

Received September 9, 2004; Revised Manuscript Received September 28, 2004

ABSTRACT: Homogeneous tandem catalysis involving a highly selective, aluminoxane-activated bis(2-decylthioethyl)amine·$CrCl_3$ complex for the synthesis of 1-hexene in tandem with a number of metallocene catalysts is discussed. Analysis by means of DSC, CRYSTAF, HT-GPC, ^{13}C NMR, and FTIR suggests that copolymers of 1-hexene and ethylene are produced with significant selectivity toward 1-hexene as comonomer. The selectivity of 1-hexene incorporation by the metallocene catalysts follows the trend in the order $[Me_2Si(2\text{-Me-Ind})_2]ZrCl_2$ > $[Me_2Si(2,3,4,5\text{-Me-Cp})(t\text{-Bu-N})]TiCl_2$ > Cp_2ZrCl_2. The highly selective nature of the ethylene trimerization catalyst employed in this study means that the industrial application of tandem catalysis is becoming increasingly viable since it approaches conventional 1-hexene LLDPE in terms of polymer microstructure control.

Background

Even though LLDPE has been in the commercial and academic domain for many decades now, both academia and industry alike are constantly faced with new challenges in this field. One such area that is experiencing renewed interest is homogeneous tandem catalysis, which in this document refers to oligomerization of ethylene and the concurrent copolymerization of the formed oligomers and ethylene. Tandem catalysis itself is not a new concept and has been well-documented in the patent literature, especially for heterogeneous systems.[1−3] There are many reasons why tandem catalysis is now receiving renewed attention. As environmental awareness and competition in commodity markets increases, chemical plants and processes are forced to reconsider their existing technology and to integrate processes previously considered separate. Specifically with regard to the commodity markets, competition will force companies to seek technologies that can facilitate faster alignment with current market trends and deliver on demand. Advances in metallocene catalysis have provided new grades of LLDPE with a better balance of mechanical and chemical properties, and these new grades challenge older existing grades of LLDPE. Finally, recent advances in selective ethylene trimerization technology have provided extremely active and selective homogeneous catalysts. The ability to combine these homogeneous technologies becomes a viable option if the properties of the polymers can be retained. In light of the above-mentioned trends, tandem catalysis seems like a very good option to consider.

By way of introduction, various heterogeneous and homogeneous tandem catalysis processes are briefly reviewed below, with specific emphasis on homogeneous tandem catalysis.

The patent literature provides a number of examples of heterogeneous tandem catalysis. Specific mention is made of the use of supported Cr(III) metal salts together with pyrrole derivatives, alkylaluminum compounds, and in some cases the addition of alkyl halides.[1−3]

Typically, a refractory metal oxide support material such as silica or alumina is impregnated with a chromium salt and calcined at a high temperature to produce a supported catalyst. Usually the calcination step is followed by a reduction step using carbon monoxide to reduce the oxidation state of the chromium catalyst from Cr(VI) to Cr(III). Following this, the supported catalyst is often treated with a silane compound such as ethylsilane. The silane treatment can be regarded as a catalyst treatment or cocatalyst and is used to produce one or more α-olefin comonomers in situ which can then be copolymerized with ethylene.

Examples of homogeneous oligomerization/copolymerization catalysis are not as well documented as the heterogeneous processes described above. Nevertheless, homogeneous tandem catalysis using binary and ternary catalyst systems have been discussed quite extensively in a number of publications by Bazan et al.[4−6] In their research, nickel, titanium, and iron oligomerization catalysts are combined with suitable polymerization catalysts to provide true homogeneous tandem catalysis. These authors specifically investigated boron derivatives as ligands for these transition metal ethylene oligomerization catalysts that specifically yield 1-butene or mixtures of α-olefins. It was claimed that these boron-based systems gave higher activity compared to conventional catalysts. An example of such a tandem catalyst combination is $\{[\eta^5\text{-}C_5Me_4)SiMe_2(\eta^1\text{-}NCMe_3)]\text{-}TiMe\}\{MeB(C_6F_5)_3\}/[(C_6H_5)_2\text{-}PC_6H_4C(OB(C_6F_5)_3)\text{-}O\kappa^2\text{-}P,O]Ni(\eta^3\text{-}CH_2C_6H_5)$.[4]

There has also been considerable interest recently in the use of bis(imino)pyridine−iron complexes as oligomerization precursors in tandem with either Ziegler−Natta catalysts or metallocene catalysts and alkylaluminum or alkoxyaluminum activators.[7,8] Because of the Schultz−Flory distribution of α-olefins produced by these oligomerization catalysts, this technology yields polymers where more than one type of α-olefin is incorporated into the polymer structure. Considerable emphasis has also been placed in this instance on the actual process of conducting tandem catalysis. For

---

* Corresponding author: e-mail deon.dewetroos@sasol.com; Fax +27 (11) 522-9737.

10.1021/ma048153k CCC: $27.50

Scheme 1 "Ideal" Proposed Mechanism for Tandem Catalysis Involving a Highly Selective Chromium-Based Ethylene Trimerization Catalyst in Tandem with a Transition-Metal-Based Polymerization Catalyst[a]

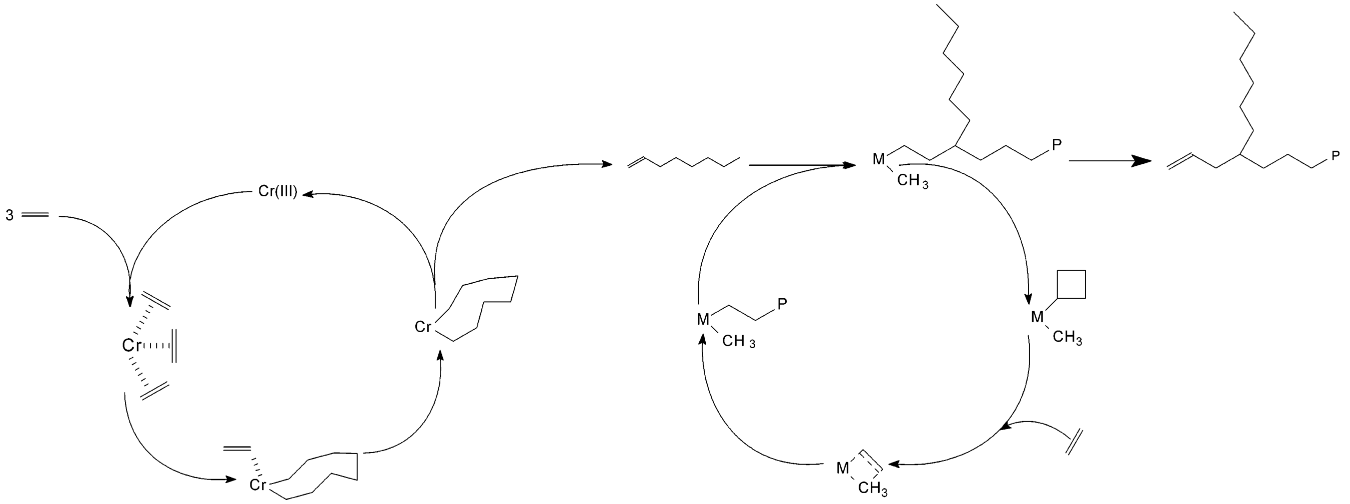

[a] M represents the transition metal of the metallocene catalyst used for polymerization.

Table 1. Melting Point, Crystallization Temperature, Polymer Yield, and Mole Percent Incorporation of 1-Hexene As Determined by ^{13}C NMR for Tandem Catalysis Reactions Using Bis(2-decylthioethyl)amine−$CrCl_3$/MAO[a]

experiment	DSC melting point (°C)	DSC crystallization point (°C)	polymer yield (g)	mol % 1-hexene incorporation
P1 (Cp_2ZrCl_2)	127	104	12.58	0.65
P2[b] ($(Me)_2Si(2\text{-}Me\text{-}Ind)ZrCl_2$)	101	66	10.15	5.81
P3 ($(Me)_2Si(4\text{-}Me\text{-}Cp)(t\text{-}Bu\text{-}N)TiCl_2$)	106 (123)	100	17.89	3.37

[a] The metallocene catalysts used are given in parentheses next to the experiment in column 1. [b] Melting point reported during first heating cycle of DSC analysis.

instance, it was recommended that a CSTR (continuous stirred tank reactor) reactor be used to enable 80% of the copolymerization to occur before the remainder of the reaction was conducted in a subsequent plug-flow reactor. It was claimed that such a polymerization process is superior since the resultant polymer contains a lot less residual monomer which can result in significant cost reduction.

Tandem catalyst systems involving more than one polymerization catalyst together with an oligomerization catalyst have also been mentioned in the patent literature.[9] In this case, two polymerization catalysts are combined with an oligomerization catalyst to produce a blend of polymers. In one example of this variation the oligomerization catalyst employed was based on an iron−bis(imino)pyridine precursor complex.[9] One of the polymerization catalysts was chosen to be relatively more effective with regard to the incorporation of α-olefins while the other polymerization catalyst is comparatively less effective at incorporation of the formed α-olefins. Both metallocene and Ziegler−Natta catalysts were utilized either in solution or coated onto a support in a slurry or in a fixed bed reactor. The polymer blend produced was designed to vary in ratio from 1:4 to 4:1 of highly crystalline polyethylene:rubbery copolymer.

The literature also provides a few examples of single homogeneous catalyst systems that exhibit a dual oligomerization/polymerization nature. One such system is $Cp^*TiMe_3-B(C_6F_5)_3$ ($Cp^* = \eta^5\text{-}C_5Me_5$).[10] The unexpected dual nature of this catalyst as both an oligomerization catalyst and a polymerization catalyst can probably be attributed to multiple oxidation states, leading to a number of possible mechanistic pathways.

Another example of such a dual functional catalyst system that is able to produce a hyperbranched low molecular mass polymer is the $TiCl_4/EtAlCl_2$ system.[11] By varying reaction conditions and the catalyst/cocatalyst ratios, the amount of branching and the molecular weight can be controlled.

Finally, there is only one account of binary homogeneous tandem catalyst systems that selectively render butyl branched polymers via the selective in situ formation of 1-hexene by one of the catalysts through ethylene trimerization. In this example British Petroleum (BP) briefly reported the use of a binary catalyst system where an aluminoxane-activated chromium−bis(phoshinoamine) catalyst selective oligomerizes ethylene to 1-hexene while the other catalyst copolymerizes ethylene and the coproduced 1-hexene.[12] Both Ziegler−Natta and metallocene catalysts were independently employed as the polymerization catalyst.

We here report a second account of binary homogeneous tandem catalyst systems that selectively render butyl-branched polymers via the selective in situ trimerization of 1-hexene by one of the two catalysts. In this instance, aluminoxane-activated bis(2-alkylsulfanylethyl)amine−$CrCl_3$, hereafter referred to as SNS catalysts,[13] is employed to trimerize 1-hexene in the presence of a metallocene copolymerization catalyst. These SNS catalysts are noteworthy as oligomerization catalysts in that they are among the most selective and active ethylene trimerization catalysts known, making them ideal candidates for use in tandem catalysis processes aimed at producing high-purity butyl-branched copolymers.

Experimental Section

All procedures were carried out under inert conditions, using predried reagents. Chemicals were obtained from Sigma-Aldrich or Boulder Scientific unless stated otherwise. All aluminoxane compounds and solutions thereof were obtained

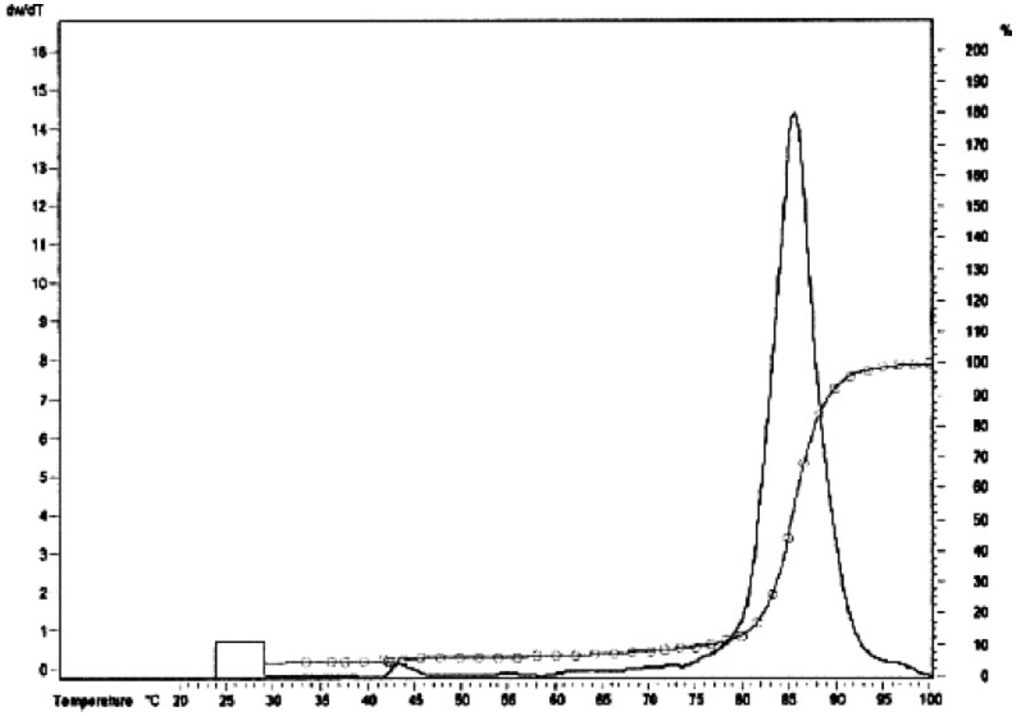

Figure 1. CRYSTAF analysis of polymer obtained from experiment P1.

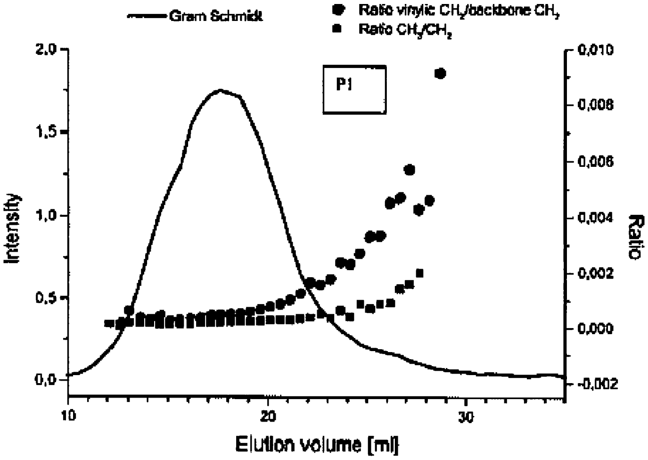

Figure 2. Gram−Schmidt elugram overlaid with the FTIR chemogram to show compositional variation with molecular mass of the polymer obtained from experiment P1.

from Crompton Gmbh, Akzo Nobel, and Albemarle Corp. The molar mass of methylaluminoxane (MAO) was taken to be 58.016 g/mol, corresponding to the (CH_3−Al−O) unit, to calculate the molar quantities of MAO used in the preparation of the catalysts described in the examples below.

Synthesis of Bis(2-decylthioethyl)amine·$CrCl_3$ Complex. Synthesis of the ligand and resultant chromium complex was conducted according to patented and published procedures under dry, inert conditions.[13,14] High-purity nitrogen gas was used to provide inert conditions. In all instances, the solvents used in all of these reactions were distilled over sodium metal and then passed through a 1 m column containing neutral alumina and tested for purity using gas chromatography.

Thus, NaOH (6 g, 150 mmol) and decylthiol (9.3 g, 150 mmol) were dissolved in anhydrous ethanol. This solution was added dropwise to a solution of bis(2-chloroethylamine) hydrochloride (8.8 g, 50 mmol) in anhydrous ethanol at a temperature of 0 °C. After addition, the solution was stirred for a further 12 h at room temperature. The solution was filtered and then evaporated to dryness. The residue remaining was dissolved in anhydrous diethyl ether and filtered to leave a colorless compound upon drying.

The colorless compound produced above was evaluated for purity by ^{1}H NMR before being dissolved in dry THF. This solution of bis(2-decylthioethyl)amine (1.06 g, 5.5 mmol) was added to a solution of $CrCl_3$·$(THF)_3$ in anhydrous THF at room temperature. The blue-green solution was stirred for an hour, after which the THF was removed by evaporation. Anhydrous diethyl ether was used to wash the dried residue. The resultant dispersion was filtered again and dried in vacuo to yield dark green crystals of [bis(2-decylthioethyl)amine]·$CrCl_3$ as confirmed by ^{1}H NMR analysis.

Examples of Tandem Catalysis. All experiments were conducted under similar dry and inert conditions as explained previously. All solvents were treated as explained previously. Experiment P1 was conducted by combining 0.026 mmol of the [bis(2-decylthioethyl)amine]·$CrCl_3$ complex (hereafter referred to as the decyl-SNS complex) with 0.0026 mmol of [bis(cyclopentadienyl)]·$ZrCl_2$ in an autoclave under nitrogen. Experiment P2 was performed by adding 0.013 mmol of [dimethylsilane(tetramethylcyclopentadienyl)(*tert*-butylamido]·$TiCl_2$ in 20 mL of toluene via an HPLC pump at a rate of 0.33 mL min^{-1} to a 300 mL Parr reactor containing 0.026 mmol of decyl-SNS complex to control the exotherm associated with polymerization.

Experiment P3 was conducted in the same way as P1 by combining 0.026 mmol of decyl-SNS complex with 0.013 mmol of dimethylsilylbis(2-methylindenyl)zirconium dichloride directly in the autoclave. Next, 300 mol equiv of methylaluminoxane (MAO, relative to the chromium metal present) was added to the reactor where after the balance of the solution in the autoclave was made up by adding anhydrous purified toluene to yield a total liquid volume of 100 mL.

During the experiments P1 and P3, the autoclave was heated to 90 °C and then pressurized to 45 bar with ethylene. Next, the ethylene supply to the reactor was terminated while the reactor temperature was maintained at 90 °C via an internal cooling coil. In the case of experiment P2, the polymerization catalyst ([dimethylsilane(tetramethylcyclopentadienyl)(*tert*-butylamido]·$TiCl_2$) was only added to the autoclave as an anhydrous toluene solution with a HPLC pump after pressurizing the reactor to 45 bar with ethylene.

DSC Analysis. Differential scanning calorimetry (DSC) analysis was performed on a Mettler Toledo DSC822 instrument by following three heating regimes. In the case of experiments P1 and P3, the polymer sample was heated from

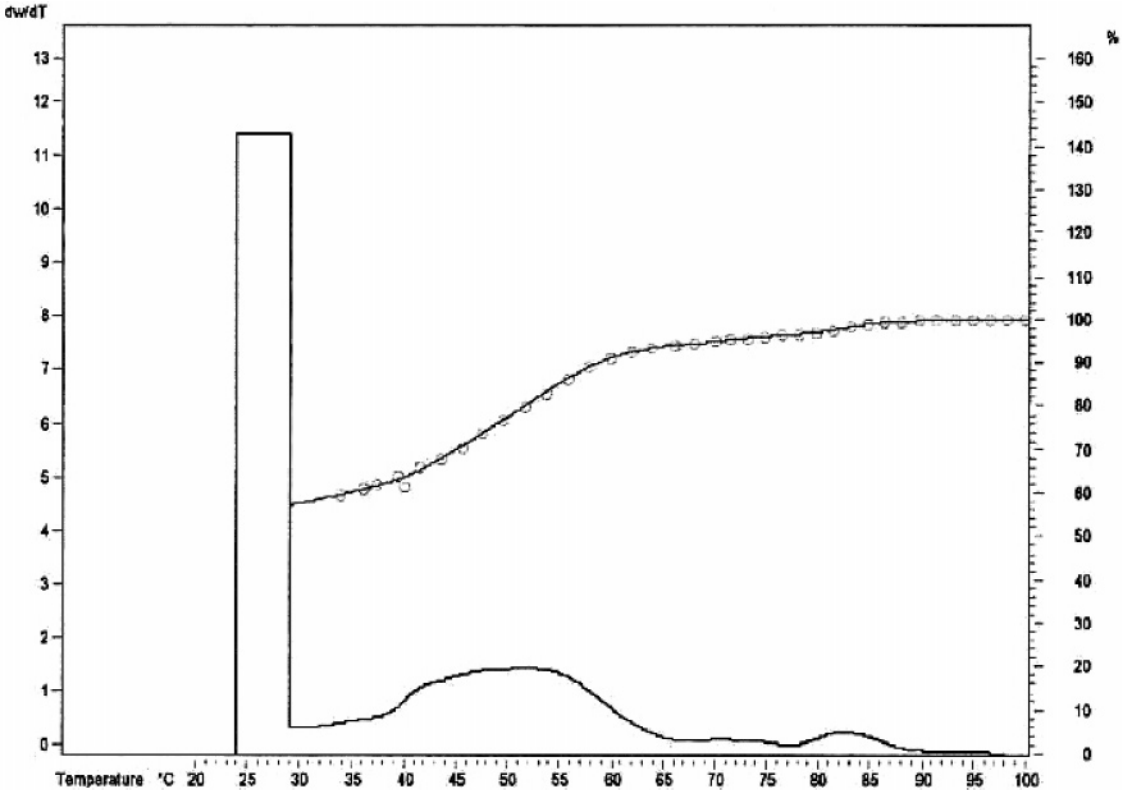

Figure 3. CRYSTAF of the polymer obtained from experiment P2.

25 to 150 °C at a rate of 10 °C min^{-1} followed by a second regime that involved cooling the polymer from 150 to 25 °C at a rate of −10 °C min^{-1}. A third regime similar to the first was then followed, and this melting point was reported. In the case of experiment P2, the method followed comprised of cooling the sample to −50 °C and heating to 150 °C at a rate of 20 °C min^{-1}. Thereafter, the sample was cooled from 150 °C at a rate of −20 °C min^{-1} to −50 °C. A third heating stage was followed by again heating from −50 to 150 °C at a heating rate of 20 °C min^{-1}.

^{13}C NMR Analysis. All spectra were collected on a Bruker Avance 500 MHz spectrometer with a 10 mm BBO probe using TCE as solvent. Samples were dissolved at 150 °C, and proton-decoupled ^{13}C spectra were collected at 120 °C using continuous decoupling and a 20 s relaxation delay with 600 scans. The methene carbon at 37.15 ppm was used for quantitative evaluation. The following ratio was used to determine the amount of 1-hexene incorporation:

$$\frac{\sum\int 2[\text{methene carbon of comonomer}]}{\sum\int[\text{backbone carbons}]}$$

CRYSTAF, HT-GPC, and GPC-FTIR Analysis. Crystallization fractionation analysis (CRYSTAF), high-temperature gel permeation chromatography (HT-GPC), and coupled gel permeation chromatography Fourier transform infrared analysis (GPC-FTIR) were conducted according to published procedures.[15]

Results and Discussion

There are a number of factors that have to taken into consideration in order to operate catalysts in tandem successfully. These include the following: (i) The catalysts should not influence each other negatively in terms of their respective catalytic functions. Ideally, the catalysts should operate in tandem but in isolation from each other with respect to reaction mechanisms and kinetics. (ii) There should be no ligand exchange between different catalysts or the existence of redox couples. (iii) The rates at which the respective catalysts operate should be comparable. (iv) The optimum conditions of each catalyst should be closely matched. (v) Ideally, the oligomerization catalysts should be highly selective toward the α-olefin being produced.

This basic set of criteria places quite severe constraints on successful tandem catalysis, especially with respect to the requirement for high oligomerization selectivity toward a single α-olefin. In this regard the highly selective SNS ethylene trimerization catalysts[13] were found to be an ideal choice. Scheme 1 details an "ideal" scenario for the operation of such a highly selective ethylene trimerization catalyst in tandem with a polymerization catalyst.

This proposed tandem mechanism probably involves a metallacycle-based oligomerization mechanism through which 1-hexene is formed in high yield and purity and the concurrent copolymerization of ethylene and 1-hexene via the classic Cossee and Arlman mechanism.

The ethyl-SNS systems are extremely active and give catalyst activities in excess of 160 000 g/(g of Cr h) with a selectivity toward 1-hexene of 98.1% at an ethylene pressure of 30 bar.[13,16] The high catalytic rates of these selective trimerization catalysts make them likely candidates for tandem catalysis since metallocene polymerization catalysts generally tend to be highly active. The viability of these SNS catalysts in tandem catalysis was assessed using a more soluble SNS precursor, namely the decyl-SNS complex. This catalyst gives similar trimerization activities to the ethyl-SNS system. The decyl-SNS catalyst was used in combination with three different metallocene catalysts, namely [$Me_2Si(2,3,4,5\text{-}Me\text{-}Cp)(t\text{-}Bu\text{-}N)]TiCl_2$, [$Me_2Si(2\text{-}Me\text{-}Ind)_2]ZrCl_2$, and Cp_2ZrCl_2.

Before conducting any tandem catalysis, a comparative study was performed to evaluate the three well-

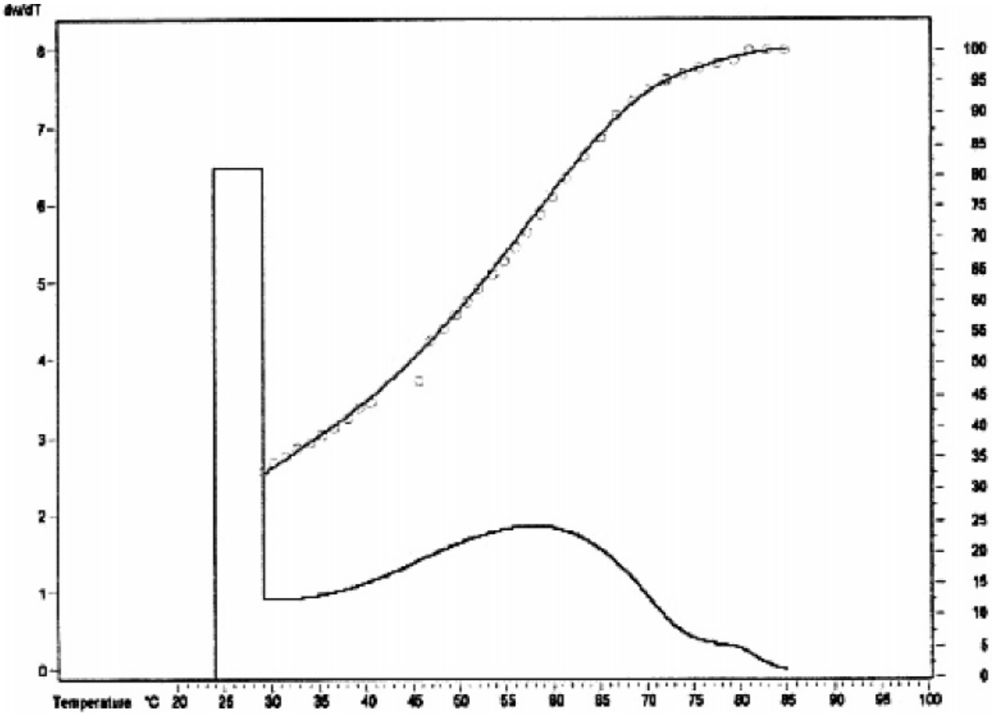

Figure 4. CRYSTAF the polymer obtained from experiment P3.

known metallocene catalysts[17] in terms of their ability to copolymerize with α-olefins. Van Reenen has reported the activities of these catalyst systems in terms of polyethylene homopolymerization.[18] The activity of Cp_2ZrCl_2 toward PE homopolymerization is reported to be approximately 34 000 kg of PE/(mol of Zr h [Et]) with the average molecular weight of the polymer being 400 000 g mol^{-1}. An activity of 40 000 kg of PE/(mol of Zr h [Et]) is reported for $[Me_2Si(2\text{-Me-Ind})_2]ZrCl_2$, which produces polymer with molecular weights averaging in the region of 200 000 g mol^{-1}. Similar activity for $[Me_2Si(2,3,4,5\text{-Me-Cp})(t\text{-Bu-N})]TiCl_2$ has been reported.[18,19] The ability to copolymerize α-olefins is reported to decrease in the order $[Me_2Si(2,3,4,5\text{-Me-Cp})(t\text{-Bu-N})]TiCl_2 > [Me_2Si(2\text{-Me-Ind})_2]ZrCl_2 > Cp_2ZrCl_2$.[17]

By comparing the melting points, crystallization points, and mol % degree of incorporation of 1-hexene provided in Table 1, it is evident that the order given above apparently does not seem to hold for these three metallocene catalysts operating in tandem with the decyl-SNS/MAO catalyst. Contrary to the published reactivity toward α-olefin copolymerization, it is evident that in the experiment where the polymerization catalyst was delivered by HPLC pump (P2) higher incorporation occurred. This may be due to the delayed activation of the metallocene catalyst since it was delivered over a period of time, and this should very likely result in a distribution of products. The reason for this assumption is based on the fact that the concentration of both the ethylene and the ratio of oligomerization catalyst to polymerization catalyst will change over time.

In the case of tandem catalysis using Cp_2ZrCl_2 (P1), very little incorporation of 1-hexene occurred. This is evident not only from the ^{13}C NMR data but also the CRYSTAF (Figure 1) and GPC–FTIR data (Figure 2) of the polymer derived from tandem catalysis involving Cp_2ZrCl_2.

Difficulty was experienced interpreting the DSC analysis of the polymer obtained from experiment P2 because no distinct peak could be obtained following the third heating stage. Only the first heating stage gave a distinct melting peak around 100 °C with a broad ill-defined melting region around 50 °C. In the case of DSC analysis of polymer obtained from experiment P3, a prominent shoulder could be detected at 123 °C in addition to the main peak at 106 °C.

To obtain more detail about the chemical composition of copolymers, CRYSTAF analysis has proved in recent years to be a valuable tool in the analytical toolbox of polymer scientists. In CRYSTAF analysis of copolymer composition, the relationship between the amount of comonomer incorporation and melting point/crystallization temperature is immediately apparent according to the following equation:[18,20]

$$T_m \cong T_m^0 - \frac{R(T_m^0)^2}{\Delta H_u} N_2 \qquad (1)$$

This equation clearly indicates that there exists a linear relationship between the melting temperature (T_m) or crystallization temperature (T_c) and the amount of comonomer (N_2) incorporated. In eq 1, ΔH_u represents the heat of fusion per polymer repeating unit, and R is the universal gas constant. T_m^0 is the melting temperature of the pure polymer.

Thus, the CRYSTAF crystallization temperature (85.7 °C) of the polymer obtained from experiment P1 is very close to that of normal HDPE (88 °C) with a small component of soluble matter being present. In addition, the HT-GPC/FTIR data of this polymer indicate that the relative concentration of methyl and vinyl groups remain virtually constant, which serves as further evidence that very little copolymerization took place. The Gram–Schmidt plot (Figure 4) is the sum of all absorptions corresponding to the concentration of the sample in the eluate. Only at the low end of the molecular weight range are deviations observed in terms of the expected branching and vinyl group ratios which are normal for chemically homogeneous polymers.

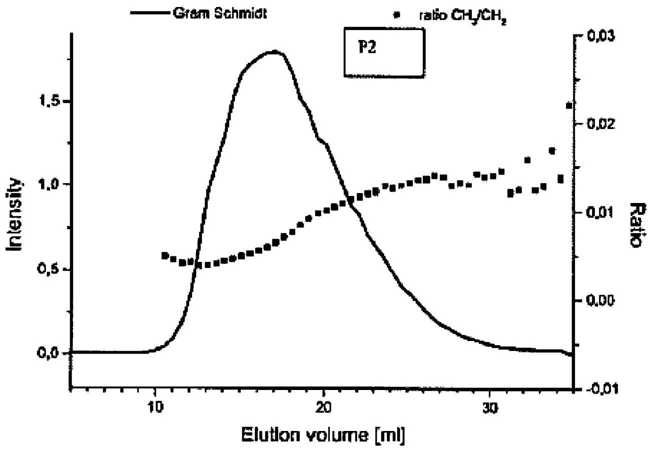

Figure 5. Gram−Schmidt elugram overlaid with the FTIR chemogram to show compositional variation with molecular mass for the polymer obtained from experiment P2.

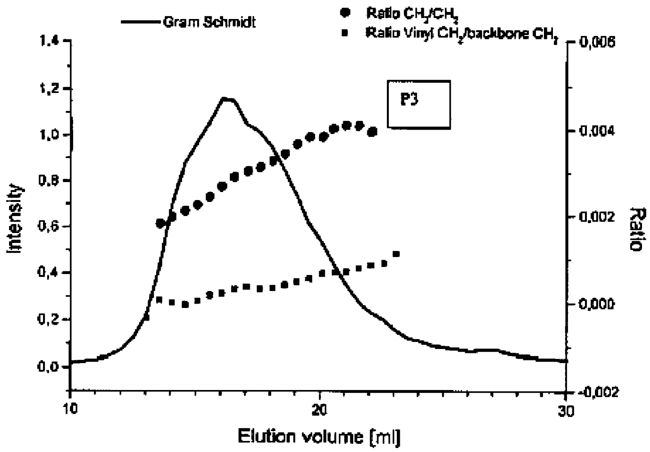

Figure 6. Gram−Schmidt elugram overlaid with the FTIR chemogram to show compositional variation with molecular mass for the polymer obtained from experiment P3.

In contrast to this, the ^{13}C NMR data (see Table 1) and CRYSTAF data (Figures 3 and 4) of the polymers from experiments P2 and P3 indicate considerable 1-hexene incorporation. Both polymer samples have no crystallization peaks above 88 °C that can be attributed to PE homopolymer formation (Figures 3 and 4). This is regardless of the rather broad chemical composition distribution of these polymers which indicates that these samples are heterogeneous in composition. The polymer obtained from experiment P2 shows a small peak around 85 °C, and this could be related to the melting point measured by DSC and reported in Table 1. However, this small peak represents a small percentage of the total polymer produced, and the majority of the polymer composition appears to be highly branched given the low crystallization temperature and high percentage soluble fraction. This compositional variance may explain the lack of a distinct melting point observed upon reheating the polymer sample during DSC analysis.

With regard to the polymer sample from experiment P3, a similar distribution is observed in the CRYSTAF analysis with a shoulder in the region of 80 °C. Again, this may account for the prominent shoulder observed during the DSC analysis (Table 1).

The Gram−Schmidt elugrams for the polymers obtained from both experiments P2 and P3 (Figures 5 and 6) indicate a clear chemical composition drift with a lower comonomer content at the high molar mass range and a higher comonomer content at the lower molar mass range. This phenomenon is indicative of the presence of copolymers.

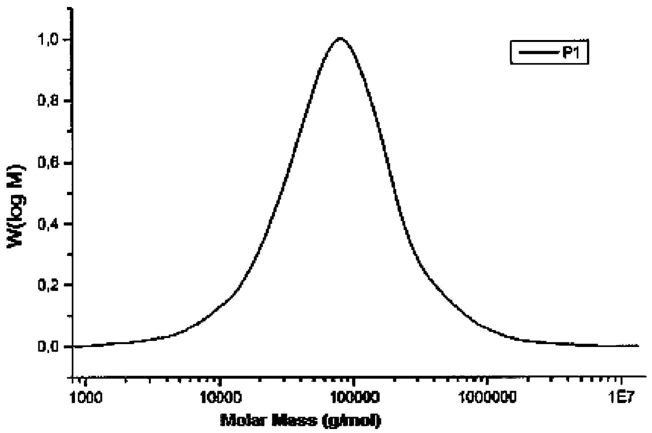

Figure 7. HT-GPC chromatogram of the polymer obtained from experiment P1.

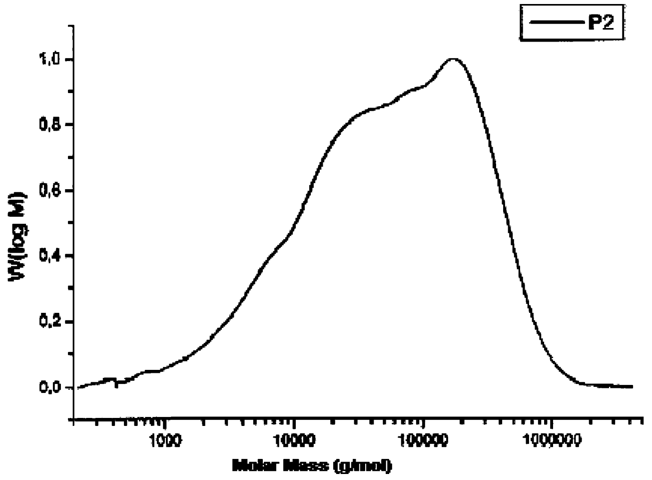

Figure 8. HT-GPC chromatogram of the polymer obtained from experiment P2.

Table 2. Relative GPC Molecular Weight Determinations

experiment	M_w (g mol^{-1})	M_n (g mol^{-1})	M_w/M_n
P1	140 000	40 000	3.53
P2	131 000	16 000	8.24
P3	154 000	56 000	2.77

Table 2 contains the number-average, weight-average, and polydispersity indices of the three polymers samples discussed above. Figures 7−9 are the molecular weight distribution curves for these samples.

The results in Table 2 indicate clearly that the addition of the polymerization catalyst by means of an HPLC pump during catalysis yields polymers with a high polydispersity (P2). This property may be beneficial in terms of polymer processing given the fact that most metallocene catalysts require more stringent downstream processing conditions due to their relatively narrow polydispersity.

The heterogeneous nature of the copolymer produced in experiment P2 is noticeable in Figure 8 by the relatively broad molecular weight distribution.

Although the polymer sample obtained from experiment P2 is polydisperse as is evident from its HT-GPC analysis (Figure 8), both polymer samples obtained from experiments P1 and P3 are relatively uniform (Figures

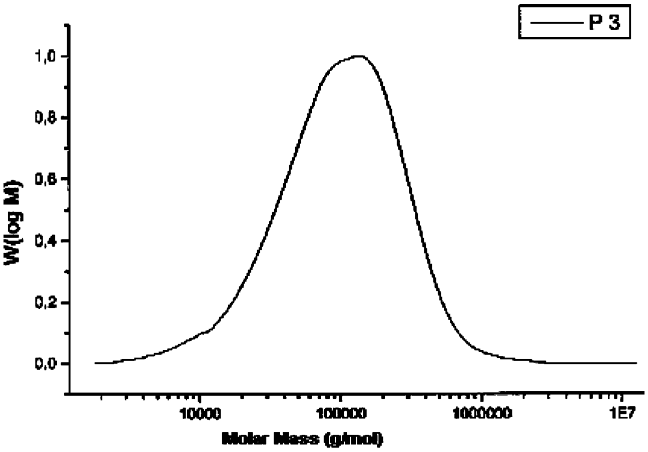

Figure 9. HT-GPC chromatogram of the polymer obtained from experiment P3.

7 and 9). One can therefore conclude that the formation of blends, except for the small amount formed in experiment P2, is not probable in the case where both the trimerization catalyst and the polymerization catalyst were combined at the beginning of the reaction. The results therefore indicate that tandem catalysis using the decyl-SNS/MAO system as trimerization catalyst in combination with suitable polymerization catalysts can indeed provide copolymers with high incorporation of 1-hexene by the careful selection of the polymerization catalyst. In addition to this, the problem of low oligomerization selectivity, a complication faced by many present day tandem catalysis systems, is circumvented by the use of this highly selective ethylene trimerization catalyst. The results of this study bring this tandem catalyst system much closer to industrial viability if one compares it to other tandem polymerization processes.

Conclusion

From the results obtained by DSC, ^{13}C NMR, HT-GPC, HT-GPC/FTRIR, and CRYSTAF analyses it is clear that successful tandem catalysis using the combination of the highly selective bis(decylsulfanyl)amine·$CrCl_3$/MAO ethylene trimerization catalyst system with a number of metallocene catalysts has been demonstrated. In the case where Cp_2ZrCl_2 was used in tandem with decyl-SNS, comparatively low copolymerization occurred. However, when $Me_2Si(2,3,4,5\text{-Me-Cp})(t\text{-Bu-N})]TiCl_2$ and $[Me_2Si(2\text{-Me-Ind})_2]ZrCl_2$ were used in tandem with decyl-SNS, copolymers with a relatively high degree of comonomer incorporation were obtained. It is further evident that, on the basis of the choice of metallocene catalyst and the mode of addition of the polymerization catalyst, copolymers with different levels of 1-hexene incorporation and overall chemical composition can be made in tandem, and this could ultimately result in polymers with different mechanical properties and commercial applications. This tandem process may therefore provide a highly attractive route toward the production of LLDPE by means of homogeneous solution polymerization.

Acknowledgment. The authors express their gratitude to SASOL Technology (Pty) Ltd. for permission to publish this work. Special thanks are extended to Mike Green for providing the facilities to conduct this work as well as Riaan Bekker, who conducted the ^{13}C NMR analysis. In addition, the work by Harald Pasch and Robert Brüll at the Deutsche Kunstoff Institut for providing the CRYSTAF, HT-GPC, and GPC-FTIR analysis is greatly appreciated.

Supporting Information Available: DSC thermograms and ^{13}C NMR spectra for the individual polymer samples. This material is available free of charge via the Internet at http://pubs.acs.org.

References and Notes

(1) Commereuc et al. US Patent No. 4,721,762, 1988.
(2) Pettijohn et al. US Patent No. 5,393,719, 1995.
(3) Reagan et al. US Patent No. 5,758,431, 1998.
(4) Kumon, Z. J. A.; Bu, X.; Bazan, G. C. *J. Am. Chem. Soc.* **2000**, *122*, 12379−12380.
(5) Kumon, Z. J. A.; Bu, X.; Bazan, G. C. *J. Am. Chem. Soc.* **2000**, *122*, 1830−1831.
(6) Quijada, R.; Rojas, R.; Bazan, G.; Kumon, Z. J. A.; Mauler, R. S.; Galland, G. S. *Macromolecules* **2001**, *34*, 2411−2417.
(7) Citron, J. D. US Patent No. 6,586,541, Du Pont, 2003.
(8) Cotts et al. US Patent No. 6,586,550, Du Pont, 2003.
(9) Wang et al. US Patent No. 6,555,631, Du Pont, 2000.
(10) Pellecchia, C.; Pappalardo, D.; Gruter, G.-J. *Macromolecules* **1999**, *32*, 4491−4493.
(11) Murtuza, S.; Harkins, S. B.; Long, G. S.; Sen, A. *J. Am. Chem. Soc.* **2000**, *122*, 1867−1872.
(12) Wass, Duncan, Frank; WO 02/04119, 2002.
(13) (a) McGuiness, D. S.; Wasserscheid, P.; Keim, W.; Morgan, D.; Dixon, J. T.; Bollmann, A.; Maumela, H.; Hess, F.; Englert, U. *J. Am. Chem. Soc.* **2003**, *125*, 5272−5273. (b) Dixon, J. T.; et al. WO 03/053890 A1, SASOL Technology (Pty) Ltd., 2003.
(14) (a) McGuiness, D. S.; Wasserscheid, P.; Keim, W.; Dixon, J. T.; Grove, J. J. C.; Hu, C.; Englert, U. *Chem. Commun.* **2003**, 334−335. (b) Dixon, J. T., et al. WO 03/053891 A1, SASOL Technology (Pty) Ltd., 2003.
(15) de Goede, S.; Brull, R.; Pasch, H.; Marshall, N. *e-Polym.* **2004**, No. 012.
(16) Dixon, J. T.; Green, M. J.; Hess, F. M.; Morgan, D. H. *J. Organomet. Chem.*, in press.
(17) (a) Kristen, M. O. *Emerging Technology Series: New & Advanced Materials* **1997**, *2/3*, 1−34. (b) Plenary lecture, 2nd Annual Unesco Training School & Poster Symposium, Sasol Auditorium, Sasol Building, Sturdee Street, Rosebank, Johannesburg, South Africa, 1999.
(18) van Reenen, A. Plenary lecture, 2nd Annual Unesco Training School & Poster Symposium, Sasol Auditorium, Sasol Building, Sturdee Street, Rosebank, Johannesburg, South Africa, 1999.
(19) McKittrick, M. W.; Jones, C. W. *J. Am. Chem. Soc., Commun.* **2003**, *126*, 3052−3053.
(20) Monrabal, B.; Blanco, J.; Nieto, J.; Soares, J. B. P. *J. Polym. Sci., Part A: Polym. Chem.* **1999**, *37*, 89−93.

MA048153K